5-[4-(1-Hydroxyethyl)phenyl]-10,15,20-triphenylporphyrin as a Probe of the Transition-State Conformation in Hydrolase-Catalyzed Enantioselective Transesterifications

Tadashi Ema,* Masahito Jittani, Kenji Furuie, Masanori Utaka, and Takashi Sakai*

Department of Applied Chemistry, Faculty of Engineering, Okayama University, Tsushima, Okayama 700-8530, Japan

ema@cc.okayama-u.ac.jp

Received September 6, 2001

5-[4-(1-Hydroxyethyl)phenyl]-10,15,20-triphenylporphyrin (**1a**) and zinc porphyrin **1b** were designed and synthesized to experimentally examine the validity of the transition-state model previously proposed for the lipase-catalyzed kinetic resolution of secondary alcohols. The lipases from *Pseudomonas cepacia* (lipase PS), *Candida antarctica* (CHIRAZYME L-2), *Rhizomucor miehei* (CHIRAZYME L-9), and *Pseudomonas aeruginosa* (lipase LIP) exhibited excellent enantioselectivity (E >100 at 30 °C). Subtilisin Carlsberg from *Bacillus licheniformis* (ChiroCLEC-BL) also showed high enantioselectivity for **1a** (E = 140 at 30 °C), and the thermodynamic parameters were determined: $\Delta\Delta H^{\ddagger} = -6.8 \pm 0.8$ kcal mol^{-1}, $\Delta\Delta S^{\ddagger} = -13 \pm 3$ cal mol^{-1} K^{-1}. Lipases and subtilisin showed *R*- and *S*-preference for **1**, respectively. The mechanisms underlying the experimental observations are explained in terms of the transition-state models. The large secondary alcohol **1** is a powerful tool for investigating the conformation of the transition state of the enzyme-catalyzed reactions. The fact that **1** was resolved with high enantioselectivity strongly suggests that the *gauche* conformation, but not the *anti* conformation, is taken in the transition state, in agreement with the transition-state models involving the stereoelectronic effect.

Introduction

The most unusual but attractive feature of lipases is that, unlike other enzymes, lipases simultaneously show high enantioselectivity and broad substrate specificity.[1] Uncovering the origin of this unique feature of lipases is an intriguing subject. Traditionally, binding interactions between enzyme's pockets and substrate's substituents are believed to be essential for enantiomer discrimination. Many binding models and active-site models have been proposed by substrate mapping,[2] and most of the computational calculations have been performed on the basis of the concept of binding models.[3] However, multisite binding interactions should necessarily restrict or narrow substrate specificity, which is opposed to the broad substrate specificity actually observed. As the number of the substrates successfully resolved by a single lipase increases enormously, mechanisms depending on binding interactions are becoming inconsistent even if drastic conformational change and different binding modes are assumed. Moreover, it should also be noted that in organic solvents, where hydrophobic interactions are unlikely to work,[4] binding interactions should be weak.

We have postulated that any specific binding interaction between an enzyme and variable regions (substituents) of substrates obstructs the simultaneous achievement of high enantioselectivity and broad substrate specificity and have demonstrated that the enantioselectivity of lipases for secondary alcohols can be accounted for even without any binding interaction. The essence of the stereo-sensing mechanism is represented in Figure 1b.[5] In this model, enantioselectivity is explained only by the conformational requirements and repulsive interactions in the transition state, and any binding interaction between enzyme's pockets and substrate's substituents is not involved. In this sense, lipases are considered to be "chemical reagent-like".[6] Further study has revealed that such a concept can be applied to subtilisins (Figure 1c).[7] These transition-state models can rationalize the opposite empirical rules for lipases (typically, *R*-preference)[8] and subtilisins (typically, *S*-preference)[7,9] (Figure 1a).

(1) For example: (a) Wong, C.-H.; Whitesides, G. M. *Enzymes in Synthetic Organic Chemistry*; Elsevier: Oxford, 1994. (b) *Enzyme Catalysis in Organic Synthesis*; Drauz, K., Waldmann, H., Eds.; VCH: New York, 1995; Vol. 1. (c) Faber, K. *Biotransformations in Organic Chemistry*; Springer-Verlag: Berlin, 1995. (d) *Enzymatic Reactions in Organic Media*; Koskinen, A. M. P., Klibanov, A. M., Eds.; Blackie Academic: Glasgow, 1996. (e) Bornscheuer, U. T.; Kazlauskas, R. J. *Hydrolases in Organic Synthesis*; Wiley-VCH: Weinheim, 1999.

(2) (a) Itoh, T.; Kuroda, K.; Tomosada, M.; Takagi, Y. *J. Org. Chem.* **1991**, *56*, 797. (b) Hultin, P. G.; Jones, J. B. *Tetrahedron Lett.* **1992**, *33*, 1399. (c) Naemura, K.; Fukuda, R.; Murata, M.; Konishi, M.; Hirose, K.; Tobe, Y. *Tetrahedron: Asymmetry* **1995**, *6*, 2385. (d) Nakamura, K.; Kawasaki, M.; Ohno, A. *Bull. Chem. Soc. Jpn.* **1996**, *69*, 1079. (e) Nishizawa, K.; Ohgami, Y.; Matsuo, N.; Kisida, H.; Hirohara, H. *J. Chem. Soc., Perkin Trans. 2* **1997**, 1293.

(3) (a) Cygler, M.; Grochulski, P.; Kazlauskas, R. J.; Schrag, J. D.; Bouthillier, F.; Rubin, B.; Serreqi, A. N.; Gupta, A. K. *J. Am. Chem. Soc.* **1994**, *116*, 3180. (b) Lemke, K.; Lemke, M.; Theil, F. *J. Org. Chem.* **1997**, *62*, 6268. (c) Grabuleda, X.; Jaime, C.; Guerrero, A. *Tetrahedron: Asymmetry* **1997**, *8*, 3675. (d) Faeffner, F.; Norin, T.; Hult, K. *Biophys. J.* **1998**, *74*, 1251. (e) Orrenius, C.; Faeffner, F.; Rotticci, D.; Öhrner, N.; Norin, T.; Hult, K. *Biocat. Biotrans.* **1998**, *16*, 1. (f) Cuiper, A. D.; Kouwijzer, M. L. C. E.; Grootenhuis, P. D. J.; Kellogg, R. M.; Feringa, B. L. *J. Org. Chem.* **1999**, *64*, 9529.

(4) Israelachvili, J. N. *Intermolecular and Surface Forces*; Academic Press: London, 1985.

(5) Ema, T.; Kobayashi, J.; Maeno, S.; Sakai, T.; Utaka, M. *Bull. Chem. Soc. Jpn.* **1998**, *71*, 443.

(6) In the field of synthetic organic chemistry, many transition-state models, which involve no binding interaction, have been proposed for various stereoselective chemical reactions. Gawley, R. E.; Aubé, J. *Principles of Asymmetric Synthesis*; Elsevier: Oxford, 1996.

10.1021/jo0109063 CCC: $22.00
Published on Web 03/01/2002

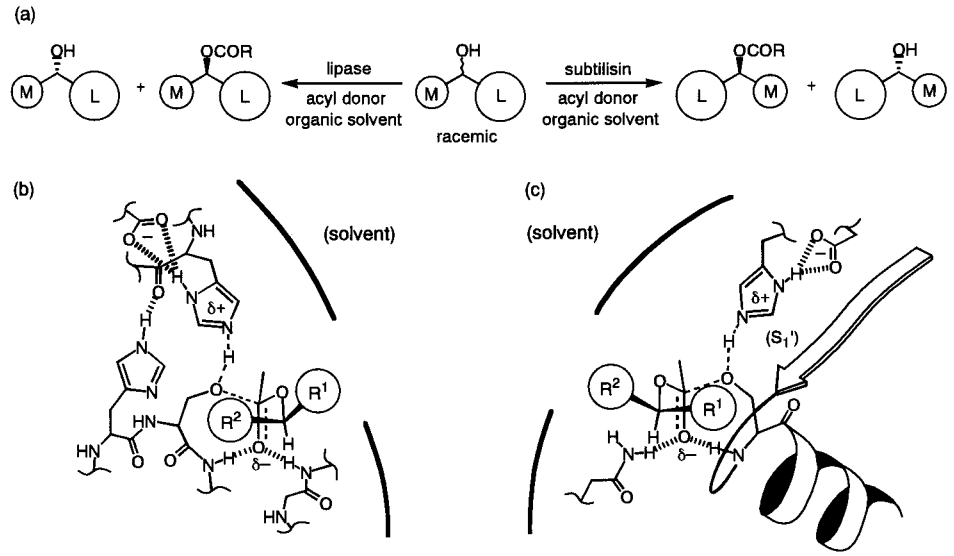

Figure 1. (a) Empirical rules for the lipase- and subtilisin-catalyzed kinetic resolutions of secondary alcohols. L and M represent the larger and smaller substituents, respectively. Typically, (*R*)- and (*S*)-enantiomers react faster in the lipase- and subtilisin-catalyzed kinetic resolutions, respectively. (b) (c) Transition-state models for the (b) lipase- and (c) subtilisin-catalyzed kinetic resolutions of secondary alcohols. In both models, (i) the C−O bond of a substrate takes the *gauche* conformation with respect to the breaking C- - -O bond, which is due to the stereoelectronic effect, and (ii) the H atom attached to the asymmetric C atom of the substrate is *syn*-oriented toward the carbonyl O atom of the acetyl group. When such a locally favorable conformation is taken, the faster-reacting enantiomer can direct the larger substituent (R^1 in (b) and R^2 in (c)) toward external solvent without severe steric hindrance, whereas the slower-reacting enantiomer directs the larger substituent (R^2 in (b) and R^1 in (c)) toward the protein wall, causing a severe steric repulsion. Even if any other conformation is taken, the slower-reacting enantiomer necessarily becomes less stable than the antipodal enantiomer. For details, see ref 5.

Chart 1

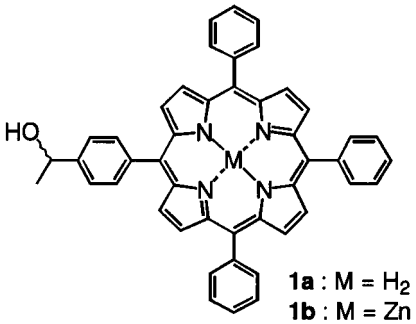

The transition-state models have been derived on the basis of the molecular orbital (MO) calculations and molecular modeling[5] and have been supported by the kinetic[5,7] and thermodynamic[10] studies. Furthermore, as reported in our preliminary papers, the extremely large secondary alcohol, 5-[4-(1-hydroxyethyl)phenyl]-10,15,-20-triphenylporphyrin (**1**) (Chart 1), undergoes lipase- and subtilisin-catalyzed transesterifications.[7,11] We designed **1** in order to investigate the conformation of the transition state. The transition-state models predict that even very large secondary alcohols whose larger substituent cannot be accommodated in any pocket of the enzymes can be efficiently resolved if they are appropriately designed, which would be difficult to predict on the basis of traditional binding models. Figure 1b and c suggests that one enantiomer of **1** ((*R*)-**1** for lipases and (*S*)-**1** for subtilisins) is susceptible to the acylation because the tetraphenylporphyrin moiety can be directed toward external solvent and that the other enantiomer ((*S*)-**1** for lipases and (*R*)-**1** for subtilisins) is highly disfavored because of the severe steric repulsion between the tetraphenylporphyrin moiety and the protein. In this paper, we report the lipase- and subtilisin-catalyzed kinetic resolutions of **1** and discuss the transition-state conformation in detail.

Results

Lipase-Catalyzed Kinetic Resolution. Porphyrin **1a** was synthesized by the condensation of benzaldehyde, 4-(1-hydroxyethyl)benzaldehyde (**3**),[12] and pyrrole according to the method of Lindsey.[13] Zinc porphyrin **1b** was prepared by the standard method with $Zn(OAc)_2$.[14] The lipase-catalyzed kinetic resolutions of **1** were performed with vinyl acetate in dry diisopropyl ether at 30 °C (Scheme 1). Several commercially available lipases were examined. The enantiomeric purities (% ee) of **1** and **2**

(7) Ema, T.; Okada, R.; Fukumoto, M.; Jittani, M.; Ishida, M.; Furuie, K.; Yamaguchi, K.; Sakai, T.; Utaka, M. *Tetrahedron Lett.* **1999**, *40*, 4367.

(8) (a) Kazlauskas, R. J.; Weissfloch, A. N. E.; Rappaport, A. T.; Cuccia, L. A. *J. Org. Chem.* **1991**, *56*, 2656. (b) Burgess, K.; Jennings, L. D. *J. Am. Chem. Soc.* **1991**, *113*, 6129. (c) Janssen, A. J. M.; Klunder, A. J. H.; Zwanenburg, B. *Tetrahedron* **1991**, *47*, 7645. (d) Xie, Z.-F. *Tetrahedron: Asymmetry* **1991**, *2*, 733.

(9) (a) Fitzpatrick, P. A.; Klibanov, A. M. *J. Am. Chem. Soc.* **1991**, *113*, 3166. (b) Wang, Y.-F.; Yakovlevsky, K.; Zhang, B.; Margolin, A. L. *J. Org. Chem.* **1997**, *62*, 3488. (c) Kazlauskas, R. J.; Weissfloch, A. N. E. *J. Mol. Catal. B: Enz.* **1997**, *3*, 65. (d) Lloyd, R. C.; Dickman, M.; Jones, J. B. *Tetrahedron: Asymmetry* **1998**, *9*, 551.

(10) Ema, T.; Yamaguchi, K.; Wakasa, Y.; Tanaka, N.; Utaka, M.; Sakai, T. *Chem. Lett.* **2000**, 782.

(11) Ema, T.; Jittani, M.; Sakai, T.; Utaka, M. *Tetrahedron Lett.* **1998**, *39*, 6311.

(12) Einhorn, J.; Einhorn, C.; Ratajczak, F.; Pierre, J.-L. *J. Org. Chem.* **1996**, *61*, 7452.

(13) Lindsey, J. S.; Schreiman, I. C.; Hsu, H. C.; Kearney, P. C.; Marguerettaz, A. M. *J. Org. Chem.* **1987**, *52*, 827.

(14) Smith, K. M. *Porphyrins and Metalloporphyrins*; Elsevier: Amsterdam, 1975.

Scheme 1

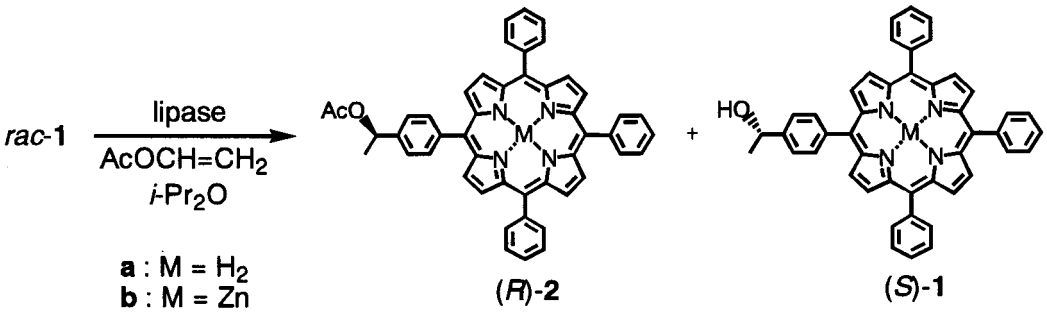

Table 1. Lipase-Catalyzed Enantioselective Transesterifications of 1[a]

					% yield[c] (% ee[d])		
entry	lipase	alcohol	time (h)	*c* (%)[b]	(*R*)-**2**	(*S*)-**1**	*E* value[e]
1	lipase PS[f]	**1a**	23	48	44 (>98)	47 (89)	>298
2	lipase PS	**1b**	23	14	12 (>98)	82 (16)	>116
3	CHIRAZYME L-2[g]	**1a**	9	50	45 (>98)	47 (>98)	>458
4	CHIRAZYME L-2	**1b**	48	20	24 (>98)	74 (25)	>126
5	CHIRAZYME L-9[h]	**1a**	48	5	8 (>98)	90 (5)	>104
6	CHIRAZYME L-9	**1b**	48	8	7 (>98)	78 (8)	>107
7	lipase LIP[i]	**1a**	5	50	46 (>98)	36 (>98)	>458
8	lipase LIP	**1b**	5	18	24 (>98)	72 (21)	>122

[a] Conditions: lipase (900 mg), **1** (42 μmol), vinyl acetate (1.3 mmol), dry *i*-Pr$_2$O (30 mL), 30 °C. [b] Conversion calculated from ee(**1**)/(ee(**1**) + ee(**2**)) according to ref 15. [c] Isolated yield. [d] Determined by HPLC (Chiralcel OD-H) after conversion to **1a**. [e] Calculated from $E = \ln [1 - c(1 + \text{ee}(\mathbf{2}))]/\ln [1 - c(1 - \text{ee}(\mathbf{2}))]$ according to ref 15. [f] *Pseudomonas cepacia* lipase (Amano Pharmaceutical). [g] *Candida antarctica* lipase (Boehringer Mannheim). [h] *Rhizomucor miehei* lipase (Boehringer Mannheim). [i] *Pseudomonas aeruginosa* lipase (Toyobo).

Scheme 2

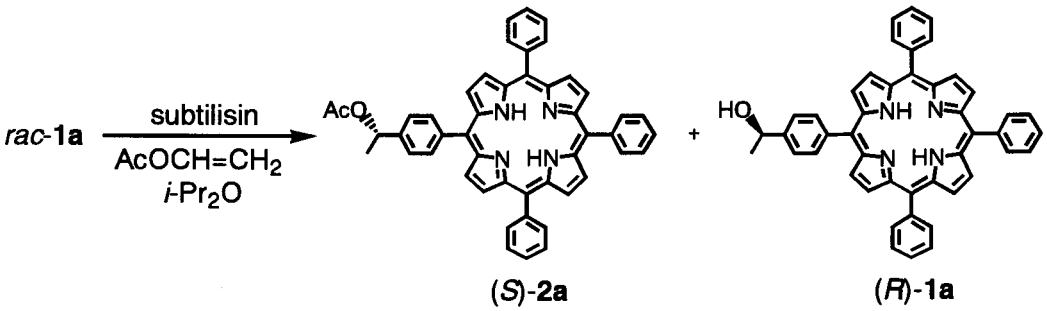

were determined by means of HPLC after they were converted to **1a**, and the *E* values were calculated according to the literature.[15] The absolute configuration of ester **2** obtained in the lipase-catalyzed transesterifications of **1** was determined to be (*R*) according to the method described in the Experimental Section. It was also confirmed by a control experiment without lipase that zinc porphyrin **1b** itself cannot function as a catalyst for the transesterification. The results are listed in Table 1. Excellent enantioselectivities ($E > 100$) were observed in all cases, and complete kinetic resolutions were achieved in entries 3 and 7, where the enantiomeric purities of both alcohol **1a** and ester **2a** were >98% ee.[16]

Subtilisin-Catalyzed Kinetic Resolution. Cross-linked enzyme crystals of subtilisin Carlsberg (Chiro-CLEC-BL) were used as a biocatalyst. The subtilisin-catalyzed kinetic resolutions of **1a** were performed with vinyl acetate in dry diisopropyl ether (Scheme 2). The (*S*)-enantiomer of **1a** was acylated faster, and a high *E* value was obtained at 30 °C (Table 2). The enantioselectivity was high but incomplete, and therefore we were able to determine the thermodynamic parameters, $\Delta\Delta H^{\ddagger}$ and $\Delta\Delta S^{\ddagger}$, according to eq 1, where $\Delta\Delta H^{\ddagger} = \Delta H^{\ddagger}_{\text{fast}} -$

Table 2. Subtilisin-Catalyzed Enantioselective Transesterifications of 1a[a]

			% yield[c] (% ee [d])		
temp (°C)	time (h)	*c* (%)[b]	(*S*)-**2a**	(*R*)-**1a**	*E* value[e]
20	3.5	45	41 (98)	54 (81)	249
25	4	38	34 (98)	61 (60)	183
30	3	42	40 (97)	57 (71)	140
35	3	42	39 (97)	59 (70)	138
40	2	37	38 (97)	59 (58)	118
45	2	37	32 (96)	68 (57)	87

[a] Conditions: ChiroCLEC-BL (40 mg), **1a** (42 μmol), vinyl acetate (1.3 mmol), dry *i*-Pr$_2$O (30 mL). [b] Conversion calculated from ee(**1a**)/(ee(**1a**) + ee(**2a**)) according to ref 15. [c] Isolated yield. [d] Determined by HPLC (Chiralpak AD). [e] Calculated from $E = \ln [1 - c(1 + \text{ee}(\mathbf{2a}))]/\ln [1 - c(1 - \text{ee}(\mathbf{2a}))]$ according to ref 15.

(15) Chen, C.-S.; Fujimoto, Y.; Girdaukas, G.; Sih, C. J. *J. Am. Chem. Soc.* **1982**, *104*, 7294.

(16) When both alcohol and ester obtained at 50% conversion are enantiomerically pure, we call the reaction "complete kinetic resolution". Many complete kinetic resolutions can be seen in the literature. See, for example: (a) Tanaka, K.; Ogasawara, K. *Synthesis* **1995**, 1237. (b) Taniguchi, T.; Takeuchi, M.; Kadota, K.; ElAzab, A. S.; Ogasawara, K. *Synthesis* **1999**, 1325. (c) Nakashima, H.; Sato, M.; Taniguchi, T.; Ogasawara, K. *Synlett* **1999**, 1754. See also ref 22. Complete desymmetrization of meso diols has also been reported and can be explained in the same way. (d) Johnson, C. R.; Golebiowski, A.; McGill, T. K.; Steensma, D. H. *Tetrahedron Lett.* **1991**, *32*, 2597.

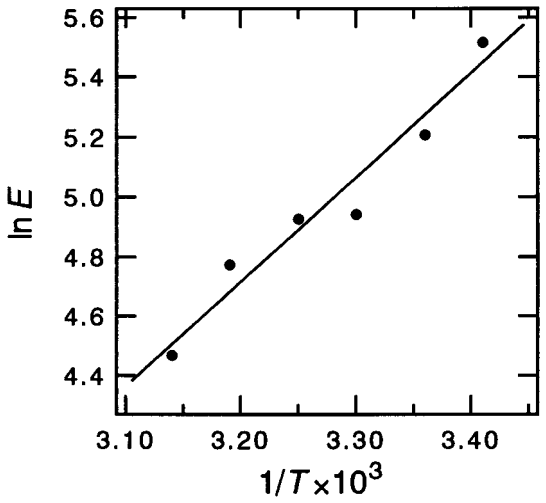

Figure 2. Plots of ln E vs $1/T$ for the subtilisin-catalyzed kinetic resolutions of **1a**.

$\Delta H^{\ddagger}_{slow}$ and $\Delta\Delta S^{\ddagger} = \Delta S^{\ddagger}_{fast} - \Delta S^{\ddagger}_{slow}$.[17]

$$\ln E = \frac{-\Delta\Delta H^{\ddagger}}{RT} + \frac{\Delta\Delta S^{\ddagger}}{R} \qquad (1)$$

The E values obtained at several temperatures are listed in Table 2. Plot of the ln E values against $1/T$ (Figure 2) afforded the following values: $\Delta\Delta H^{\ddagger} = -6.8 \pm 0.8$ kcal mol^{-1}, $\Delta\Delta S^{\ddagger} = -13 \pm 3$ cal mol^{-1} K^{-1}. Previously, we have found a linear relationship between the $\Delta\Delta H^{\ddagger}$ and $\Delta\Delta S^{\ddagger}$ values for the subtilisin-catalyzed kinetic resolutions of a variety of secondary alcohols.[10] Interestingly, the one set of the data for **1a** was found to fall into this linear relationship (Figure 3).[18]

Discussion

Four kinds of lipases exhibited excellent enantioselectivity and *R*-preference for **1** (Table 1), as predicted by the transition-state model. To our knowledge, **1** is the largest secondary alcohol that has been successfully resolved by the lipase-catalyzed reactions. The X-ray crystal structures of lipases from *Pseudomonas cepacia*,[19] *Candida antarctica*,[20] and *Rhizomucor miehei*,[21] which are used in the present study, are available from the Protein Data Bank. Obviously, the tetraphenylporphyrin moiety of **1** is so large (edge-to-edge distance of ca. 17 Å) that it cannot be accommodated by any pocket of these enzymes. Therefore, the results in Table 1 strongly suggest that the accommodation of the larger substituent of substrates in a pocket of the enzymes is not necessarily required for attaining high enantioselectivity. In entries 3 and 7 (Table 1), the transesterification reactions

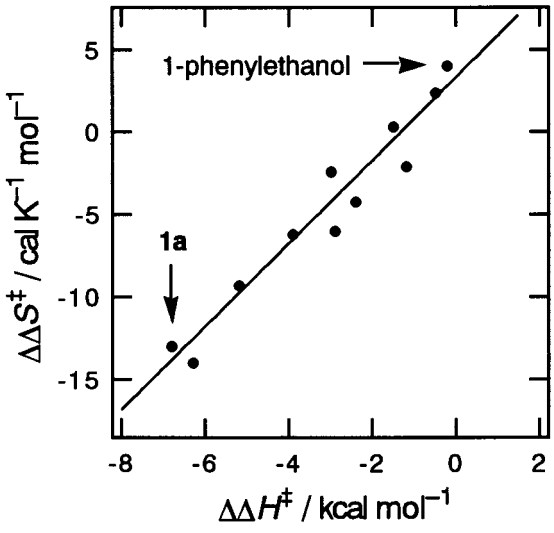

Figure 3. A linear relationship between $\Delta\Delta H^{\ddagger}$ and $\Delta\Delta S^{\ddagger}$ values in the subtilisin-catalyzed kinetic resolutions of a variety of secondary alcohols. Except for **1a**, all the data are taken from ref 10. For comparison, the data for 1-phenylethanol is indicated.

stopped completely at 50% conversion and never proceeded further even after a prolonged reaction time.[16] This observation indicates that the high enantioselectivity is achieved by the highly suppressed reactivity of the (*S*)-enantiomer. Figure 1b suggests that a severe steric repulsion occurs between the tetraphenylporphyrin moiety of the slower-reacting enantiomer, (*S*)-**1**, and the protein. Thus, the transition-state model proposed by us contrasts with traditional binding models, in the latter of which binding interactions between pockets of an enzyme and substituents of a faster-reacting enantiomer are the principal factor in reaction acceleration and high enantioselectivity.

Interestingly, zinc porphyrin **1b** was acylated more slowly than free base porphyrin **1a** in most cases (Table 1). We suppose that **1b** binds to polar amino acid residues on the protein surface. This coordination may block the active site or may decrease the protein flexibility essential to catalytic activity. Because it is well-known that a porphyrin ring is rigidified by complexation with a metal atom, the increased rigidity of **1b** might also be related to the reduced reactivity. Even free base porphyrin **1a** reacted relatively slowly in most cases, e.g., the total turnover number (TTN) of the enzyme at 50% conversion in entry 1 was calculated to be ca. 77, which is much lower than ca. 5000 reported for 2-[(*N*,*N*-dimethylcarbamoyl)methyl]-3-cyclopenten-1-ol under the similar reaction conditions.[22] Computer modeling suggested that even (*R*)-**1a** can cause unfavorable steric interactions with some parts of the protein such as the lid (not shown). The reactivity of **1** may also be lowered apparently by the low concentration of **1** (1.4 mM) or inherently by the large size of the molecule.

Subtilisin Carlsberg showed *S*-preference for **1a** (Table 2), which is opposite to the *R*-preference of lipases. It is known that an approximate mirror-image relationship exists between the catalytic residues (the catalytic triad and the oxyanion hole) of the serine proteases and those

(17) (a) Phillips, R. S. *Trends Biotechnol.* **1996**, *14*, 13. (b) Sakai, T.; Kawabata, I.; Kishimoto, T.; Ema, T.; Utaka, M. *J. Org. Chem.* **1997**, *62*, 4906. (c) Sakai, T.; Kishimoto, T.; Tanaka, Y.; Ema, T.; Utaka, M. *Tetrahedron Lett.* **1998**, *39*, 7881.

(18) The reaction conditions for **1a** are slightly different from those for secondary alcohols in ref 10. When molecular sieves 4Å were added, less reliable data with larger standard deviations were obtained: $\Delta\Delta H^{\ddagger} = -6.6 \pm 1.2$ kcal mol^{-1}, $\Delta\Delta S^{\ddagger} = -12 \pm 4$ cal mol^{-1} K^{-1}.

(19) Kim, K. K.; Song, H. K.; Shin, D. H.; Hwang, K. Y.; Suh, S. W. *Structure* **1997**, *5*, 173. The name of *Pseudomonas cepacia* has been changed to *Burkholderia cepacia*.

(20) Uppenberg, J.; Hansen, M. T.; Patkar, S.; Jones, T. A. *Structure* **1994**, *2*, 293.

(21) Derewenda, U.; Brzozowski, A. M.; Lawson, D. M.; Derewenda, Z. S. *Biochemistry* **1992**, *31*, 1532.

(22) Ema, T.; Maeno, S.; Takaya, Y.; Sakai, T.; Utaka, M. *J. Org. Chem.* **1996**, *61*, 8610.

of lipases.[23] The opposite enantiopreferences of subtilisin (*S*-preference) and lipases (*R*-preference) are reasonable because the enantioselectivity results predominantly from the local conformational requirements and repulsive interactions in the transition state (Figure 1b and c).

Previously, we have observed a clear tendency that subtilisin shows an enantioselectivity for various secondary alcohols lower than that of lipases.[7] We have ascribed the reduced enantioselectivity of subtilisin to the lack of a protein wall corresponding to the "triangular wall" of lipases, which we had proposed to be important for high enantioselectivity of lipases.[5] Instead of such a wall, subtilisin has a shallow depression (S_1'),[24] which is made up of the β-strand, the α-helical turn, and the histidine imidazole of the catalytic triad and which is open to external solvent (Figure 1c).[25] Owing to this depression (S_1'), the steric repulsion point in subtilisin is distant from the stereocenter of a secondary alcohol in the transition state as compared to the case of lipases. Besides, the active site of subtilisin is less hindered than that of lipases having a lid. As a result of these structural differences, subtilisin allowed the unfavorable enantiomer, (*R*)-**1a**, to react very slowly, resulting in the high but incomplete enantioselectivity (Table 2), whereas lipases completely blocked the reaction of (*S*)-**1**, leading to the enantiospecific kinetic resolutions (Table 1).

We have previously observed a partial compensation effect between the $\Delta\Delta H^{\ddagger}$ and $\Delta\Delta S^{\ddagger}$ values for subtilisin-catalyzed kinetic resolutions of a variety of secondary alcohols.[10] As shown in Figure 3, the $\Delta\Delta S^{\ddagger}$ value decreases with a decrease in the $\Delta\Delta H^{\ddagger}$ value. Equation 1 indicates that a negative $\Delta\Delta H^{\ddagger}$ value contributes to an increase in the *E* value, whereas a negative $\Delta\Delta S^{\ddagger}$ value contributes to a decrease in the *E* value. We have explained this phenomenon in terms of the transition-state model (for details, see ref 10). Interestingly, the present thermodynamic data for **1a** also falls into this linear relationship (Figure 3). This suggests that the extremely large alcohol **1a** is enantiodiscriminated basically in the same way as for other secondary alcohols of smaller sizes. The *E* value for **1a** ($E = 140$) is much larger than, for example, that for 1-phenylethanol ($E = 10$).[7] Figure 3 indicates that this enhanced *E* value for **1a** is due to the large, negative $\Delta\Delta H^{\ddagger}$ value, which in turn suggests a large difference in the degree of the steric repulsion and the strain caused in the transition state between the enantiomers of **1a**.

Because the stereoelectronic effect originates from the intrinsic nature of chemical bonds,[26] it should be retained not only in chemical reactions but also in enzymatic reactions.[27] Figure 4 illustrates that the *gauche* conformation, with the lone-pair orbital (n) mixing with the antibonding orbital (σ^*), facilitates the C−O bond cleavage more efficiently than the *anti* conformation and that the protein is flanked by the substrate part (R) more closely in the *gauche* conformation than in the *anti*

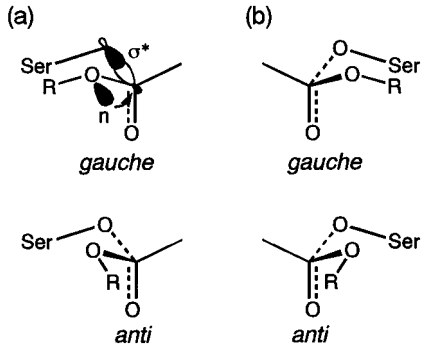

Figure 4. Conformations of the transition state liberating an ester product in the (a) lipase- and (b) subtilisin-catalyzed acylations of a secondary alcohol (ROH). In both cases, the protein core is on the rear side of the paper, and on the front side of the paper is external solvent. The *gauche* and *anti* conformations are defined by the dihedral angle between the R−O bond and the breaking C- - -O bond. The *gauche* conformation is more favorable than the *anti* conformation because of the stereoelectronic effect (see text or ref 5).

conformation. As can be seen in the transition-state models (Figure 1b and c), this conformational requirement due to the stereoelectronic effect plays a key role in chiral discrimination.[5] On the other hand, studies based on an X-ray crystal structure of a lipase complexed with a chiral transition-state analogue, menthyl phosphonate,[3a] or based on molecular mechanics (MM) calculations on tetrahedral intermediates[3d−f] have failed to find the significance of the stereoelectronic effect, and the researchers seem to believe (i) the *anti* conformation is the reactive conformation and (ii) binding pockets are essential for chiral discrimination. Truly, the tetrahedral geometry at the P atom (phosphonate inhibitor) or at the central C atom (tetrahedral intermediate) and the electronegative O atom locally mimic the transition-state structure of the esterification/hydrolysis. However, it is doubtful whether even the conformation mimics the real transition state. The stereoelectronic effect in the P-containing complex must be small, because the long P−O bond distance and the differences in orbital size and energy level between the P and O atoms weaken the n−σ^* orbital mixing,[28] and because the complex is in the ground state.[29] The stereoelectronic effect in the tetrahedral intermediate is also small as reported previously.[5,29] The large alcohol **1** is a powerful tool to address this conformational issue. In particular, subtilisin Carls-

(23) Derewenda, Z. S.; Wei, Y. *J. Am. Chem. Soc.* **1995**, *117*, 2104.

(24) The S_1' subsite was originally defined as a binding region for the leaving group of peptide substrates. Schechter, I.; Berger, A. *Biochem. Biophys. Res. Commun.* **1967**, *27*, 157.

(25) (a) Neidhart, D. J.; Petsko, G. A. *Protein Eng.* **1988**, *2*, 271. (b) McPhalen, C. A.; James, M. N. G. *Biochemistry* **1988**, *27*, 6582.

(26) (a) Deslongchamps, P. *Stereoelectronic Effects in Organic Chemistry*; Pergamon: Oxford, 1983. (b) Kirby, A. J. *Stereoelectronic Effects*; Oxford University Press: Oxford, 1996.

(27) Dugas, H. *Bioorganic Chemistry: A Chemical Approach to Enzyme Action*, 3rd ed.; Springer-Verlag: New York, 1996.

(28) The X-ray crystal structures of lipase-inhibitor complexes in the Protein Data Bank show that the dihedral angle in question (C−O−P−O_γ) varies widely, although there is a weak tendency to fall into the *gauche* conformation: 91.4° (1EX9), 124.9° (1HQD), 140.0° (5LIP), 75.4° (1LPB), 130.3° (1LPM), 70.8° (1LPS), 94.1° (4TGL), and 70.5° (5TGL).

(29) To simulate the enantioselectivity, many researchers have employed the tetrahedral intermediate, instead of the real transition state, in the MM calculations. However, it has been revealed by the MO calculations that the stereoelectronic effect operates effectively in the bond-breaking/forming transition state rather than in the tetrahedral intermediate.[5] The energetic benefit due to the stereoelectronic effect is inherently small in the tetrahedral intermediate and probably in the enzyme−phosphonate complex because they have no transiently breaking/forming chemical bond. Moreover, the MM calculations cannot properly evaluate the stereoelectronic effect that explicitly involves the interactions of molecular orbitals. For these reasons, the real transition state should be treated by MO methods. As an alternative method, Tafi et al. have involved the concept of the stereoelectronic theory in the MM calculations on the tetrahedral intermediates to reproduce the enantiopreference of a lipase. Tafi, A.; van Almsick, A.; Corelli, F.; Crusco, M.; Laumen, K. E.; Schneider, M. P.; Botta, M. *J. Org. Chem.* **2000**, *65*, 3659.

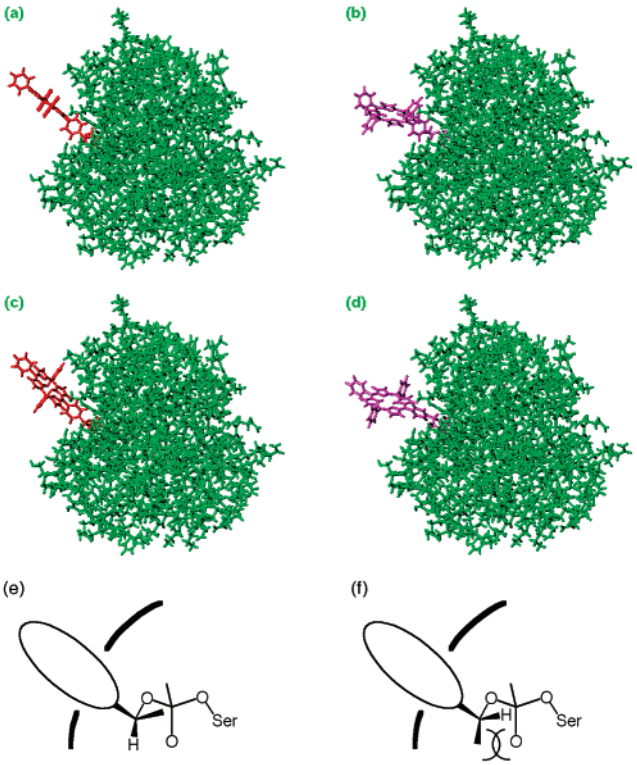

Figure 5. Comparison of the *gauche* and *anti* conformations in the subtilisin-catalyzed transesterification of **1a**. (a) The *anti* conformation for (*S*)-**1a**. (b) The *anti* conformation for (*R*)-**1a**. (c) The *gauche* conformation for (*S*)-**1a**. (d) The *gauche* conformation for (*R*)-**1a**. The enzyme is shown in green, (*S*)-**1a** is in red, and (*R*)-**1a** is in magenda. The orientation of the protein is similar to that in Figure 1c. Close-up representations of (c) and (d) are drawn in (e) and (f), respectively, where the tetraphenylporphyrin moiety is shown by an ellipse. In (a), (b), (c), and (e), the H atom attached to the asymmetric C atom of **1a** is *syn*-oriented toward the oxyanion, which is conformationally favorable. In the case of (d) and (f), the tetraphenylporphyrin moiety is forced to point outside, with the methyl group *syn*-oriented toward the oxyanion, which is conformationally unfavorable due to the torsional strain and the steric repulsion.[5] These structures are shown to help the readers understand the discussion, and it is only for easy manipulations that we employed the tetrahedral intermediate. Because the stereoelectronic effect in the tetrahedral intermediate is small, the tetrahedral intermediate cannot be a substitute for the real transition state. See refs 5 and 29.

berg, whose active site is much less crowded than that of lipases, provides a clear argument. If the *anti* conformation is allowed, the tetraphenylporphyrin moiety of both enantiomers makes no contact with the protein in such a conformation that the H atom attached to the asymmetric C atom of **1a** is *syn*-oriented toward the oxyanion (Figure 5a and b). This will result in no enantioselectivity. In contrast, when the *gauche* conformation is taken, the tetraphenylporphyrin moiety of (*S*)-**1a** can be favorably directed toward external solvent (Figure 5c and e), whereas (*R*)-**1a** undergoes a steric repulsion and/or a strain considerably (Figure 5d and f). This can lead to differential activation energy. Clearly, the facts that the high *E* value ($E = 140$ at 30 °C) and the large, negative $\Delta\Delta H^{\ddagger}$ value (-6.8 kcal mol^{-1}) were observed for **1a** strongly support the *gauche* conformation.[30]

Conclusion

Despite their extreme simplicity, the transition-state models are indeed consistent with several experimental observations for lipases and subtilisins. They can clearly explain (i) the simultaneous achievement of high enantioselectivity and broad substrate specificity,[5] (ii) the opposite enantiopreferences of lipases and subtilisins for secondary alcohols,[5,7] (iii) low activity for secondary alcohols having bulky substituents on both sides,[5] (iv) little or no activity for tertiary alcohols,[5] and (v) the reason the large alcohol **1** can be resolved with high enantioselectivity.[7,11] In this paper, the experimental observations for the enzyme-catalyzed kinetic resolutions of **1** have been explained in detail in terms of the transition-state models. By using **1** as a substrate, it has been experimentally supported that the chemical reagent-like feature of the enzymes (conformational requirements and repulsive interactions in the transition state) is the determinant of the enantioselectivity and that the *gauche* conformation is taken in the transition state. It can therefore be predicted that artificial catalysts mimicking the catalytic machinery of lipases and subtilisins will show *R*- and *S*-preference, respectively, for a variety of secondary alcohols. The transition-state models are so useful that they will enable us to plan efficient chemoenzymatic syntheses and rational alteration of the enzymes.

Experimental Section

Materials and Methods. Silica gel and basic alumina column chromatography was performed using Fuji Silysia BW-127 ZH (100−270 mesh) and Merck aluminum oxide 90 active basic (0.063−0.200 mm), respectively. Thin-layer chromatography (TLC) was performed on Merck silica gel 60 F_{254}. Lipase PS (1% (w/w) powder) was provided by Amano Pharmaceutical Co. CHIRAZYME L-2 (carrier-fixed C2, isoform B) and L-9 (lyo) were provided by Boehringer Mannheim GmbH. Lipase LIP and ChiroCLEC-BL were purchased from Toyobo Co. and Altus Biologics Inc, respectively. 4-(1-Hydroxyethyl)benzaldehyde (**3**) was prepared according to the literature.[12] Dry diisopropyl ether and dry Et_2O were distilled from sodium, and dry CH_2Cl_2 was distilled from CaH_2. The enantiomeric purities of **1a**, **2a**, **3**, **5**, and **6** were determined by HPLC using Chiralcel OD-H (**1a**), Chiralpak AD (**1a**, **2a**, **5**, **6**), and Chiralcel OB (**3**) columns (Daicel Chemical Industries); that of **7** was determined by capillary gas chromatography using a CP-cyclodextrin-β-2,3,6-M-19 column (Chrompack, ϕ 0.25 mm × 25 m).^{1}H and ^{13}C NMR spectra measured in $CDCl_3$ at 200 and 50 MHz, respectively, are reported.

Computer Modeling. Molecular modeling was performed with SYBYL 6.4 (Tripos, Inc.) on an O2 workstation (Silicon Graphics, Inc.). The X-ray crystal structures of lipases from *P. cepacia* (1OIL),[19] *C. antarctica* (1LBS),[20] and *R. miehei* (4TGL)[21] and that of subtilisin Carlsberg (2SEC)[25b] available from the Protein Data Bank were used. After an inhibitor and water molecules were removed, the tetrahedral intermediate for (*R*)- or (*S*)-**1a** was constructed, and the hydrogen atoms

(30) We also examined three kinds of lipases (1OIL, 1LBS, 4TGL). Because the active site of the lipases is very crowded, it is surprising indeed that **1** was allowed to react. Visual inspection of the tetrahedral intermediates indicated that (*R*)-**1a** can direct the tetraphenylporphyrin moiety toward external solvent in a locally favorable conformation shown in Figure 1b, although even this conformation obviously suffered to some degree from a steric repulsion with the peripheral protein parts, which can explain the low TTN (see text). The *anti* conformation of (*R*)-**1a** and both conformations of (*S*)-**1a** had the tetraphenylporphyrin moiety unacceptably overlapped with the protein or underwent a severe strain. Accordingly, (*R*)-**1a** most likely takes the *gauche* conformation in the transition state, and (*S*)-**1a** seems to have no way to overcome the high energy barrier.

were generated. The conformation was manually adjusted appropriately. The active site of the lipases was too crowded to perform a reliable calculation. Since the active site of subtilisin Carlsberg is not so crowded, the MM calculations were performed. The whole protein was treated as a rigid body using Aggregates, and the remaining parts were allowed to move using the Tripos force field and the Gasteiger−Hückel charges. The obtained structures were then compared.

5-[4-(1-Hydroxyethyl)phenyl]-10,15,20-triphenylporphyrin (1a). To a solution of **3** (602 mg, 4.01 mmol), benzaldehyde (1.27 g, 12.0 mmol), and pyrrole (1.10 g, 16.4 mmol) in dry CH_2Cl_2 (1.5 L) was added $BF_3{\cdot}OEt_2$ (224 mg, 1.58 mmol) under N_2. After the solution was stirred at room temperature for 3.5 h in the dark, *o*-chloranil (2.73 g, 11.1 mmol) was added. After being stirred for 1 h, the solution was concentrated to ca. 100 mL and washed with saturated aqueous $NaHCO_3$ (100 mL × 2). The organic layer was separated and dried over Na_2SO_4. After the solution was concentrated, the product was purified by repeated silica gel and basic alumina column chromatography (hexane/$CHCl_3$/EtOAc (20:20:3)) to afford **1a** as a purple solid (175 mg, 7%): mp > 280 °C; ^{1}H NMR δ −2.61 (br s, 2H), 1.79 (d, J = 6.4 Hz, 3H), 2.13 (br s, 1H), 5.19 (q, J = 6.4 Hz, 1H), 7.70−7.82 (m, 11H), 8.23−8.34 (m, 8H), 8.96 (s, 8H); ^{13}C NMR δ 25.4, 70.3, 119.9, 120.2, 123.7, 126.7, 127.7, 131.1, 134.5, 134.7, 141.2, 142.1, 145.0; IR (KBr) 3428, 3318 cm^{-1}; HR FAB-MS calcd for $C_{46}H_{35}N_4O$ 659.2811, found 659.2775; Anal. Calcd for $C_{46}H_{34}N_4O$: C, 83.87; H, 5.20; N, 8.50. Found: C, 83.61; H, 5.10; N, 8.39.

{5-[4-(1-Hydroxyethyl)phenyl]-10,15,20-triphenylporphyrinato}zinc(II) (1b). To a solution of **1a** (122 mg, 185 μmol) in $CHCl_3$ (50 mL) was added a solution of $Zn(OAc)_2{\cdot}2H_2O$ (433 mg, 1.97 mmol) in MeOH (10 mL). The solution was heated at reflux for 30 min. The progress of the reaction was monitored by UV−vis spectroscopy. After brine (100 mL) was added to the solution, the organic layer was separated, dried over Na_2SO_4, and concentrated. Recrystallization from $CHCl_3$/hexane afforded **1b** as purple crystals (99 mg, 74%): mp > 280 °C; ^{1}H NMR δ 1.69 (d, J = 6.3 Hz, 3H), 1.89 (br s 1H), 5.04−5.14 (m, 1H), 7.63−7.77 (m, 11H), 8.16−8.24 (m, 8H), 8.95 (s, 8H); ^{13}C NMR δ 25.3, 70.4, 120.8, 121.1, 123.6, 126.5, 127.5, 132.0, 134.4, 134.6, 142.0, 142.8, 144.7, 150.2; IR (KBr) 3413 cm^{-1}; HR FAB-MS calcd for $C_{46}H_{33}N_4OZn$ 721.1946, found 721.1902.

Lipase-Catalyzed Kinetic Resolutions of 1. To a mixture of **1a** (28 mg, 42 μmol) or **1b** (30 mg, 42 μmol) and lipase (900 mg) in dry *i*-Pr_2O (30 mL) was added vinyl acetate (112 mg, 1.30 mmol) at 30 °C. The mixture was stirred at ca. 450 rpm in the dark. The progress of the reaction was monitored by TLC. The mixture was filtered and concentrated. Alcohol (*S*)-**1** and ester (*R*)-**2** were separated by silica gel column chromatography (hexane/$CHC1_3$/EtOAc (28:16:3) to (20:20:3)). (*R*)-**2a**: mp 270−273 °C; ^{1}H NMR δ −2.76 (br s, 2H), 1.85 (d, J = 6.6 Hz, 3H), 2.28 (s, 3H), 6.27 (q, J = 6.6 Hz, 1H), 7.71−7.78 (m, 11H), 8.21−8.26 (m, 8H), 8.87 (s, 8H); ^{13}C NMR δ 21.6, 22.5, 72.3, 119.6, 120.2, 124.4, 126.7, 127.7, 131.1, 134.6, 134.7, 141.1, 141.7, 142.1, 170.6; IR (KBr) 3319, 1727 cm^{-1}; HR FAB-MS calcd for $C_{48}H_{37}N_4O_2$ 701.2917, found 701.2871. (*R*)-**2b**: mp 273−275 °C; ^{1}H NMR δ 1.83 (d, J = 6.6 Hz, 3H), 2.23 (s, 3H), 6.22 (q, J = 6.6 Hz, 1H), 7.70−7.79 (m, 11H), 8.19−8.25 (m, 8H), 8.96 (s, 8H); ^{13}C NMR δ 21.5, 22.5, 72.3, 120.6, 121.1, 124.3, 126.5, 127.5, 132.0, 134.4, 134.5, 140.8, 142.3, 142.8, 150.1, 150.2, 170.6; IR (KBr) 1736 cm^{-1}; HR FAB-MS calcd for $C_{48}H_{35}N_4O_2Zn$ 763.2051, found 763.2087. HPLC for **1a**: Chiralcel OD-H, hexane/2-PrOH = 9:1, flow rate 0.5 mL/min, detection 420 nm, (*R*) 27.2 min, (*S*) 32.2 min. The enantiomeric purities of **2a**, **2b**, and **1b** were determined after conversion to **1a**.

Subtilisin-Catalyzed Kinetic Resolutions of 1a. General procedure for the subtilisin-catalyzed kinetic resolutions of **1a** is similar to that for the lipase-catalyzed kinetic resolutions. After a mixture of **1a** (28 mg, 42 μmol) and ChiroCLEC-BL (40 mg) in dry *i*-Pr_2O (30 mL) was stirred for 30 min in a water bath thermostated at the reaction temperature, vinyl acetate (112 mg, 1.30 mmol) was added. The mixture was stirred at ca. 450 rpm in the dark. The progress of the reaction was monitored by TLC. The mixture was filtered and concentrated. Alcohol (*R*)-**1a** and ester (*S*)-**2a** were separated by silica gel column chromatography as shown above. HPLC for **1a**: Chiralpak AD, hexane/2-PrOH = 92:8, flow rate 0.3 mL/min, detection 420 nm, (*R*) 54.0 min, (*S*) 66.4 min. HPLC for **2a**: Chiralpak AD, hexane/2-PrOH = 98:2, flow rate 0.3 mL/min, detection 420 nm, (*R*) 67.1 min, (*S*) 81.9 min.

Scheme 3[a]

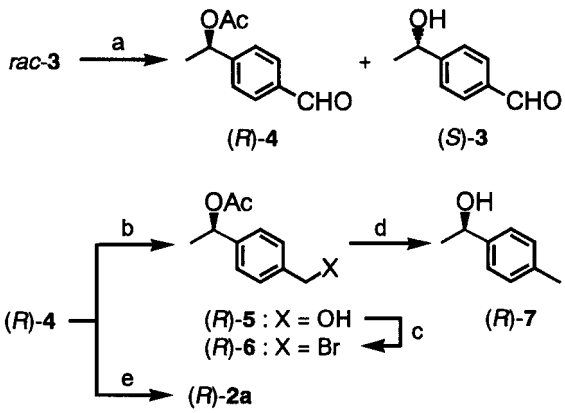

[a] Reagents and conditions: (a) CHIRAZYME L-2, vinyl acetate, *i*-Pr_2O, −10 °C; (b) $NaBH_4$, EtOH, 0 °C to rt; (c) CBr_4, PPh_3, CH_2Cl_2, 0 °C to rt; (d) $LiAlH_4$, Et_2O, 0 °C to rt; (e) pyrrole, PhCHO, $BF_3{\cdot}OEt_2$, CH_2Cl_2, rt, then *o*-chloranil.

Determination of Absolute Configuration. The absolute stereochemistry of **1** and **2** was established according to Scheme 3. The absolute configuration of ester **4** obtained in the lipase-catalyzed kinetic resolution of **3** was determined to be (*R*) by confirming that **4** was converted to (*R*)-**7**, whose specific rotation has been reported.[31] This result agrees with the prediction by the transition-state model that (*R*)-**4** will be obtained. The authentic (*R*)-**4** was converted to (*R*)-**2a**. By comparing the HPLC retention times, the absolute configuration of **2a** obtained in the lipase-catalyzed kinetic resolution of **1a** was determined to be (*R*). Detailed procedures are described below.

(*R*)-4-(1-Acetoxyethyl)benzaldehyde ((*R*)-4).[32] After a mixture of **3** (301 mg, 2.00 mmol) and CHIRAZYME L-2 (667 mg) in dry *i*-Pr_2O (6.7 mL) was stirred at −10 °C for 10 min, vinyl acetate (345 mg, 4.01 mmol) was added. After being stirred at −10 °C for 3 h, the mixture was filtered and concentrated. Alcohol (*S*)-**3** and ester (*R*)-**4** were separated by silica gel column chromatography (hexane/EtOAc (4:1) to (3:1)). (*R*)-**4**: 40% yield, >98% ee; $[\alpha]^{25}_D$ = +119 (*c* 1.04, $CHCl_3$); ^{1}H NMR δ 1.54 (d, J = 6.6 Hz, 3H), 2.10 (s, 3H), 5.90 (q, J = 6.6 Hz, 1H), 7.50 (d, J = 8.2 Hz, 2H), 7.87 (d, J = 8.2 Hz, 2H), 10.0 (s, 1H); ^{13}C NMR δ 21.1, 22.2, 71.7, 126.4, 130.0, 135.8, 148.4, 170.1, 191.7; IR (neat) 1738, 1704 cm^{-1}. (*S*)-**3**: 53% yield, 71% ee; $[\alpha]^{25}_D$ = −36.5 (*c* 1.25, $CHCl_3$), lit.[33] $[\alpha]^{24}_D$ = +50.2 (*c* 3.11, $CHCl_3$) for (*R*)-**3** with 88% ee (the absolute configuration reported as a tentative assignment in ref 33 was found to be correct). HPLC for **3**: Chiralcel OB, hexane/2-PrOH = 95:5, flow rate 0.5 mL/min, detection 254 nm, (*S*) 35.9 min, (*R*) 41.3 min. The enantiomeric purity of **4** was determined after conversion to **3**.

(*R*)-4-(1-Acetoxyethyl)benzyl Alcohol ((*R*)-5). To a solution of (*R*)-**4** (480 mg, 2.50 mmol) in EtOH (10 mL) and saturated aqueous $NaHCO_3$ (0.4 mL) was added portionwise $NaBH_4$ (47 mg, 1.24 mmol) at 0 °C over 5 min. After the mixture was stirred at room temperature for 1.5 h, brine (3 mL) was added. After being stirred for 20 min, the solution was concentrated and extracted with Et_2O (6 mL × 6). The organic layer was dried over Na_2SO_4 and concentrated. The

(31) Kitayama, K.; Uozumi, Y.; Hayashi, T. *J. Chem. Soc., Chem. Commun.* **1995**, 1533.
(32) Salomon, R. G.; Reuter, J. M. *J. Am. Chem. Soc.* **1977**, *99*, 4372.
(33) Soai, K.; Hori, H.; Kawahara, M. *Tetrahedron: Asymmetry* **1990**, *1*, 769.

product was purified by silica gel column chromatography (Et_2O) to afford (*R*)-**5** as a colorless oil (303 mg, 62%, >98% ee): bp 76 °C (4 mmHg); $[\alpha]^{26}_D = +124$ (*c* 1.02, EtOH); ^{1}H NMR δ 1.52 (d, $J = 6.6$ Hz, 3H), 2.04 (s, 3H), 2.37 (br s, 1H), 4.63 (s, 2H), 5.85 (q, $J = 6.6$ Hz, 1H), 7.33 (s, 4H); ^{13}C NMR δ 21.2, 22.1, 64.7, 72.1, 126.2, 127.0, 140.6, 140.9, 170.4; IR (neat) 3418, 1737 cm^{-1}; MS (EI) *m*/*z* 194 (M^+). HPLC: Chiralpak AD, hexane/2-PrOH = 95:5, flow rate 0.5 mL/min, detection 254 nm, (*R*) 23.4 min, (*S*) 27.2 min.

(*R*)-4-(1-Acetoxyethyl)benzyl Bromide ((*R*)-6). To a solution of (*R*)-**5** (254 mg, 1.31 mmol) and CBr_4 (650 mg, 1.96 mmol) in dry CH_2Cl_2 (6.5 mL) was added portionwise PPh_3 (516 mg, 1.97 mmol) at 0 °C over 5 min. The solution was stirred at room temperature for 3.5 h. The solvent was removed under reduced pressure. The products were dissolved in Et_2O and filtered (3 mL × 5). The filtrate was concentrated under reduced pressure. Purification by silica gel column chromatography (hexane/Et_2O (5:1)) afforded (*R*)-**6** as a colorless oil (313 mg, 93%, >98% ee): bp 50 °C (4 mmHg); $[\alpha]^{26}_D = +99.1$ (*c* 1.10, EtOH); ^{1}H NMR δ 1.52 (d, $J = 6.6$ Hz, 3H), 2.07 (s, 3H), 4.48 (s, 2H), 5.87 (q, $J = 6.6$ Hz, 1H), 7.32 (d, $J = 8.6$ Hz, 2H), 7.38 (d, $J = 8.6$ Hz, 2H); ^{13}C NMR δ 21.3, 22.1, 33.1, 71.8, 126.5, 129.2, 137.3, 141.9, 170.2; IR (neat) 1732 cm^{-1}; MS (EI) *m*/*z* 256, 258 (M^+). Anal. Calcd for $C_{11}H_{13}O_2Br$: C, 51.38; H, 5.10. Found: C, 51.54; H, 5.23. HPLC: Chiralpak AD, hexane/2-PrOH = 95:5, flow rate 0.3 mL/min, detection 254 nm, (*R*) 17.1 min, (*S*) 20.7 min.

(*R*)-1-(*p*-Tolyl)ethanol ((*R*)-7). To a suspension of $LiAlH_4$ (28 mg, 0.74 mmol) in dry Et_2O (3 mL) was added dropwise a solution of (*R*)-**6** (128 mg, 0.50 mmol) in dry Et_2O (2 mL) under N_2 at 0 °C over 5 min. The mixture was stirred at room temperature for 2 h. EtOAc (0.5 mL) was added dropwise at 0 °C over 5 min, and the mixture was stirred for 20 min. After brine (1 mL) was added to the mixture, the organic layer was separated. The aqueous layer was extracted with Et_2O (3 mL × 5). The combined organic layer was dried over Na_2SO_4 and concentrated. Purification by silica gel column chromatography (hexane/Et_2O (4:1)) afforded (*R*)-**7** as a colorless oil (48 mg, 70%, >99% ee): bp 47 °C (5 mmHg); $[\alpha]^{29}_D = +57.8$ (*c* 1.10, $CHCl_3$), lit.[31] $[\alpha]^{25}_D = +44.7$ (*c* 1.27, $CHCl_3$) for (*R*)-**7** with 89% ee; ^{1}H NMR δ 1.48 (d, $J = 6.5$ Hz, 3H), 2.11 (br s, 1H), 2.36 (s, 3H), 4.85 (q, $J = 6.5$ Hz, 1H), 7.17 (d, $J = 8.1$ Hz, 2H), 7.27 (d, $J = 8.1$ Hz, 2H); ^{13}C NMR δ 21.0, 25.0, 70.1, 125.3, 129.1, 137.0, 142.8; IR (neat) 3358 cm^{-1}; MS (EI) *m*/*z* 136 (M^+). GC: CP-cyclodextrin-β-2,3,6-M-19, injection temperature 280 °C, column temperature 120 °C, detection temperature 220 °C, carrier gas He, (*R*) 13.1 min, (*S*) 14.1 min.

(*R*)-5-[4-(1-Acetoxyethyl)phenyl]-10,15,20-triphenylporphyrin ((*R*)-2a). To a solution of (*R*)-**4** (98 mg, 0.51 mmol), benzaldehyde (161 mg, 1.52 mmol), and pyrrole (135 mg, 2.01 mmol) in dry CH_2Cl_2 (200 mL) was added $BF_3{\cdot}OEt_2$ (28 mg, 0.20 mmol). After the mixture was stirred at room temperature for 3 h in the dark, *o*-chloranil (339 mg, 1.38 mmol) was added. After being stirred for 1 h, the solution was concentrated to ca. 50 mL and washed with saturated aqueous $NaHCO_3$ (15 mL). The organic layer was separated, dried over $MgSO_4$, and concentrated. The product was purified by repeated silica gel column chromatography (hexane/$CHCl_3$/EtOAc (2:1:0) to (10:5:2)) to afford (*R*)-**2a** as a purple solid (43 mg, 12%, >98% ee).

Acknowledgment. We are grateful to Amano Pharmaceutical Co. and Boehringer Mannheim GmbH for providing us with lipase PS and CHIRAZYME L-2, L-9, respectively. We are grateful to the SC-NMR Laboratory of Okayama University and the MS Laboratory of Faculty of Agriculture, Okayama University for the measurements of NMR and mass spectra, respectively. We also thank Mr. T. Nitoda and Mr. K. Murai for the measurement of HR FAB-MS and EI-MS, respectively. This work was partially supported by a Grant-in-Aid for Scientific Research from the Ministry of Education, Science, Sports and Culture of Japan.

Supporting Information Available: ^{1}H and ^{13}C NMR spectra for **1a**, **1b**, **2a**, **2b**, and **3**−**7**. This material is available free of charge via the Internet at http://pubs.acs.org.

JO0109063